Systematics of the average L-shell ionization probability in K-shell ionizing collisions by light ions

R. L. Watson, B. I. Sonobe,* J. A. Demarest,† and A. Langenberg

Cyclotron Institute and Department of Chemistry, Texas A&M University, College Station, Texas 77843

(Received 31 July 1978)

The apparent average L-shell ionization probabilities in K-shell ionizing collisions by He, C, O, and Ne ions incident on Al, Si, and Cl targets at relative velocities ranging from 2 to 8.5 have been determined from high-resolution $K\alpha$ x-ray measurements. These data, in combination with data from previous work, enabled a detailed examination of the dependence of the single K- plus multiple L-shell ionization process on projectile and target atomic number, and on relative velocity. The He-ion-on-Al data are compared with the results of binary-encounter approximation and semiclassical approximation calculations, and a general semiempirical scaling law is deduced for light-ion collisions.

I. INTRODUCTION

Numerous studies of $K\alpha$ x-ray satellite production by energetic ions have been carried out in recent years. As a result of this activity, a body of data encompassing a wide range of bombarding energies and projectile-target combinations has accumulated. The purpose of the present work is twofold: (i) to test current theoretical descriptions of single K- plus multiple L-shell ionization in ion-atom collisions in greater detail and over a more extensive energy range than has been done previously, and (ii) to examine the systematic behavior of the average L-shell ionization probability in K-shell ionizing collisions $(\bar{p}_L)$ by light ions $(Z \sim 1$ to 3) as a function of projectile energy and target atomic number.

Experimental measurements have been performed to supplement the data already existing in the literature. In particular, the previous measurements of Richard *et al.*[1] (0.4–3.0-MeV He on Al) have been extended up to 40.5 MeV and the previous measurements of Knudson *et al.*[2] (1.5–15-MeV Ne on Al) have been extended up to 112.6 MeV. Data are also presented for He on Si, Cl, and Ti targets. Additional measurements were carried out on Al and Si targets using carbon and oxygen ions to enable a detailed examination of the projectile atomic number (Z_1) dependence of the single K- plus multiple L-shell ionization process.

The He-on-Al data are compared with the results of calculations using the binary-encounter approximation (BEA)[3] and the semiclassical approximation (SCA).[4] A new prescription for incorporating the binding energy increases accompanying multiple L-electron ejection into the BEA calculation is described and compared with the experimental data. Furthermore, the data resulting from the present work in combination with

other data from the literature provide a basis for a semiempirical representation of $\bar{p}_L$ in terms of a "universal" velocity function.

II. EXPERIMENTAL METHODS AND RESULTS

Beams of $^4\text{He}^{2+}$, $^{12}\text{C}^{3+}$, $^{16}\text{O}^{3+}$, and $^{20}\text{Ne}^{4+}$ were provided by the Texas A & M variable energy cyclotron. The details of the beam handling system are the same as described in Ref. 5. The flat crystal Bragg spectrometer system used to measure the spectra of $K\alpha$ x rays has also been described previously (Ref. 5). A PET (pentaerythritol) crystal was employed for the Al and Si measurements, a NaCl crystal for the Cl measurements and a LiF crystal for the Ti measurement. Target specifications were as follows: Al—2.3-mg/cm² foils, Si—0.92–1.71-mg/cm² SiO vacuum evaporated onto Al foils, Cl-1.05-mg/cm² NaCl vacuum evaporated onto an Al foil, and Ti—0.45-mg/cm² Ti vacuum evaporated onto an Al foil.

Additional measurements were performed on gaseous and solid Si, S, and Cl targets using a sealed-gas-cell system and curved-crystal spectrometer to check for electron-rearrangement effects. The details of this spectrometer and the gas-target system are described in Ref. 6.

The relative intensities f_n of the KL^n satellite peaks observed in the present He-ion measurements are listed in Table I. These relative intensities were extracted from the spectra using a least-squares peak-fitting procedure and have been corrected for absorption and for detection efficiency using the methods described in Ref. 5. Also given in Table I is the experimental $\bar{p}_L$, which is the apparent average L-shell ionization probability in K-shell ionizing collisions obtained using the relationship

WATSON, SONOBE, DEMAREST, AND LANGENBERG

TABLE I. Results of $K\alpha$ x-ray satellite measurements using He ions.

Target	$\bar{E}$ [a] (MeV)	f_n $n=0$	$n=1$	$n=2$	$\bar{p}_L$
Al	4.9	0.580	0.336	0.084	0.063 ± 0.003
	6.1	0.643	0.285	0.064	0.052 ± 0.003
	10.0	0.761	0.208	0.032	0.034 ± 0.003
	22.9	0.865	0.135		0.017 ± 0.003
	40.5	0.895	0.105		0.013 ± 0.003
SiO(Si)	4.6	0.529	0.382	0.089	0.070 ± 0.003
	6.6	0.630	0.317	0.053	0.053 ± 0.003
	10.1	0.753	0.219	0.029	0.035 ± 0.003
NaCl(Cl)	5.1	0.623	0.329	0.048	0.053 ± 0.003
	6.4	0.663	0.298	0.039	0.047 ± 0.003
	10.4	0.749	0.232	0.019	0.034 ± 0.003
	24.3	0.874	0.117	0.009	0.017 ± 0.003
	29.9	0.888	0.112		0.014 ± 0.003
	40.5	0.904	0.096		0.012 ± 0.003
Ti	5.4	0.739	0.261		0.033 ± 0.003

[a] Average beam energy for the detection of $K\alpha$ x rays as determined using the procedures described in Ref. 5.

$$\bar{p}_L = \frac{\bar{n}}{8} = \frac{1}{8} \sum_{n=1}^{7} n f_n, \tag{1}$$

where n is the number of missing L-shell electrons associated with each satellite peak and 8 is the maximum number of L-shell vacancies possible. The term "apparent" is applied to the experimental $\bar{p}_L$ since an exact determination of

TABLE II. Results of $K\alpha$ x-ray satellite measurements using C, O, and Ne ions.

Target	$\bar{E}$ [a] (MeV)	f_n $n=0$	$n=1$	$n=2$	$n=3$	$n=4$	$n=5$	$n=6$	$\bar{p}_L$
Carbon ions									
Al	9.4	0.029	0.120	0.337	0.292	0.161	0.061		0.327 ± 0.003
	18.5	0.058	0.181	0.377	0.251	0.105	0.029		0.282 ± 0.003
	23.6	0.078	0.219	0.396	0.223	0.084			0.252 ± 0.003
	40.3	0.177	0.318	0.344	0.129	0.033			0.190 ± 0.003
	72.3	0.316	0.360	0.324					0.126 ± 0.003
SiO(Si)	9.8	0.027	0.151	0.308	0.304	0.138	0.073		0.324 ± 0.003
	18.8	0.061	0.238	0.377	0.235	0.087			0.256 ± 0.003
	24.8	0.076	0.274	0.352	0.277	0.071			0.243 ± 0.003
	41.2	0.172	0.373	0.304	0.127	0.024			0.182 ± 0.003
	72.9	0.350	0.438	0.213					0.108 ± 0.003
Oxygen ions									
Al	18.4	0.034	0.101	0.319	0.304	0.180	0.061		0.335 ± 0.003
	25.2	0.047	0.118	0.315	0.289	0.164	0.067		0.328 ± 0.003
	33.8	0.057	0.133	0.351	0.284	0.141	0.035		0.303 ± 0.003
Si	6.4	0.024	0.108	0.237	0.298	0.181	0.114	0.037	0.374 ± 0.003
	18.1	0.029	0.117	0.252	0.289	0.169	0.108	0.034	0.364 ± 0.003
	25.2	0.038	0.131	0.270	0.285	0.153	0.091	0.033	0.348 ± 0.003
	44.5	0.066	0.192	0.303	0.256	0.109	0.051	0.023	0.299 ± 0.003
SiO(Si)	6.7	0.022	0.110	0.258	0.304	0.176	0.108	0.022	0.364 ± 0.003
	22.4	0.029	0.130	0.286	0.303	0.152	0.082	0.018	0.342 ± 0.003
	26.1	0.039	0.144	0.295	0.292	0.138	0.072	0.020	0.334 ± 0.003
	28.2	0.040	0.146	0.292	0.292	0.139	0.070	0.021	0.329 ± 0.003
	31.4	0.041	0.159	0.305	0.290	0.126	0.065	0.014	0.319 ± 0.003
	38.1	0.049	0.177	0.321	0.276	0.109	0.052	0.016	0.305 ± 0.003
	52.9	0.079	0.229	0.333	0.233	0.076	0.034	0.018	0.271 ± 0.003
Neon ions									
Al	17.8	0.032	0.081	0.254	0.289	0.220	0.124		0.370 ± 0.003
	34.1	0.055	0.089	0.278	0.279	0.196	0.103		0.348 ± 0.003
	112.6	0.142	0.226	0.332	0.216	0.070	0.011		0.235 ± 0.003
SiO(Si)	19.8	0.021	0.092	0.221	0.281	0.189	0.143	0.053	0.395 ± 0.003
	36.6	0.040	0.106	0.247	0.286	0.172	0.112	0.037	0.366 ± 0.003
	114.1	0.121	0.253	0.330	0.211	0.069	0.017		0.238 ± 0.003

[a] Average beam energy for the detection of $K\alpha$ x-rays as determined using the procedures described in Ref. 5.
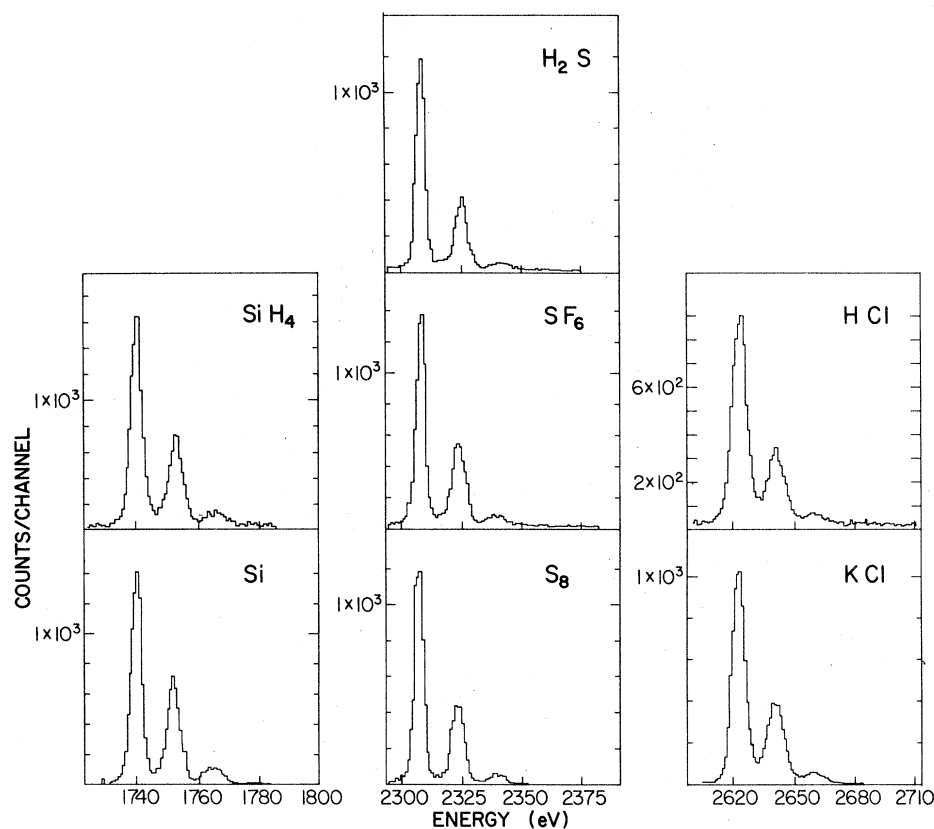
FIG. 1. $K\alpha$ x-ray spectra for several gaseous and solid compounds of Si, S, and Cl using 6.7-MeV helium ions.

this probability must take into account the variation of the fluorescence yield (including the effect of vacancy rearrangement) for each state of *L*-shell ionization. The results of the carbon-, oxygen-, and neon-ion measurements are presented in Table II.

The gas-solid comparative measurements mentioned above were carried out with 6.7-MeV He ions to ascertain the extent to which the original vacancy distribution created in the collision is altered by electron rearrangement processes occurring prior to $K\alpha$ x-ray emission in light-

ion collisions. This effect has been found to be relatively important in heavy-ion collisions and gives rise to a 15% reduction in the $\bar{p}_L$ value for Si in going from gaseous SiH_4 to solid Si with 32-MeV oxygen ions.[5,6] A comparison of the $K\alpha$ x-ray spectra obtained with several gaseous and solid compounds of Si, S, and Cl is shown in Fig. 1 and the results of these measurements are given in Table III. The various spectra for a given element are nearly identical despite the differences in chemical environment and physical state. This indicates that fast electron rearr-

TABLE III. Comparison of $K\alpha$ x-ray satellite relative intensities for various solid and gaseous compounds of Si, S, and Cl using 6.7-MeV He ions.

Compound	$\bar{E}$ [a] (MeV)	$n=0$	f_n $n=1$	$n=2$	$\bar{p}_L$	$\bar{p}_{L\,(\text{corr})}$ [b]
Si(s)	4.9	0.572	0.366	0.062	0.061 ± 0.003	0.051
$SiH_4(g)$	4.8	0.616	0.327	0.057	0.055 ± 0.003	0.044
$S_8(s)$	4.9	0.623	0.333	0.044	0.053 ± 0.003	0.043
$SF_6(g)$	5.1	0.611	0.345	0.044	0.054 ± 0.003	0.045
$H_2S(g)$	4.8	0.652	0.312	0.036	0.049 ± 0.003	0.038
KCl(Cl)(s)	5.0	0.627	0.315	0.058	0.052 ± 0.003	0.042
HCl(g)	4.9	0.654	0.295	0.051	0.050 ± 0.003	0.039

[a] Average beam energy for the detection of $K\alpha$ x rays as determined using the procedures described in Ref. 5.
[b] Corrected for projectile energy loss (i.e., $\bar{p}_L$ value for 6.7-MeV He ions).

TABLE IV. Apparent average L-shell ionization probabilities in K-shell ionizing collisions by light ions.

Target	Projectile	$v_1/\bar{v}_L$ [a]	$\bar{p}_L$ [b]	Ref.
Al	$^1H^+$	2.10	0.027	7
	$^4He^{2+}$	0.81	0.094	1
		0.99	0.126	
		1.14	0.140	
		1.28	0.144	
		1.40	0.144	
		1.51	0.140	
		1.61	0.134	
		1.71	0.128	
		1.80	0.120	
		1.89	0.114	
		1.98	0.110	
		2.06	0.106	
		2.13	0.100	
		2.21	0.096	
		2.82	0.063	Present work
		3.17	0.052	
		3.27	0.050	8
		4.04	0.034	Present work
		5.55	0.017	
		8.11	0.013	
Si	$^1H^+$	2.10	0.019	7
	$^4He^{2+}$	2.38	0.070	Present work
		2.85	0.053	
		3.51	0.035	
P	$^1H^+$	2.10	0.017	7
S	$^1H^+$	2.10	0.015	7
	$^4He^{2+}$	1.92	0.053	Present work
Cl	$^1H^+$	2.10	0.011	7
	$^4He^{2+}$	1.79	0.053	Present work
		2.01	0.047	
		2.61	0.034	
		3.91	0.017	
		4.34	0.014	
		5.04	0.012	
Ar	$^1H^+$	1.33	0.015	9
		1.69	0.013	
		1.84	0.010	
		2.35	0.008	
	$^4He^{2+}$	1.59	0.044	Present work
Ca	$^1H^+$	1.00	0.011	7
		1.09	0.011	10
		2.10	0.007	7
	$^2H^+$	1.49	0.010	11
		1.86	0.009	
		2.07	0.007	
		3.33	0.003	
		4.30	0.002	
	$^4He^{2+}$	1.09	0.042	10
		1.49	0.042	11
		1.86	0.034	
		2.06	0.025	
		3.04	0.013	
		3.33	0.012	
		3.85	0.009	
		4.30	0.008	
Sc	$^1H^+$	1.00	0.010	7
		1.01	0.010	10
	$^4He^{2+}$	1.01	0.038	10
Ti	$^1H^+$	0.95	0.009	10
		1.00	0.009	7
		1.68	0.007	12
		1.99	0.006	
		2.13	0.005	
	$^2H^+$	1.30	0.009	11
		2.10	0.006	
		2.19	0.005	
		2.66	0.004	
		3.76	0.002	
	$^4He^{2+}$	0.95	0.031	10
		1.06	0.033	12
		1.23	0.033	Present work
		1.30	0.037	11
		1.60	0.028	12
		1.62	0.031	11
		1.81	0.030	
		1.82	0.023	
		2.66	0.015	11
		2.91	0.013	
	$^7Li^{3+}$	1.31	0.075	12
		1.63	0.058	
		1.85	0.053	
		2.09	0.043	
V	$^1H^+$	0.90	0.005	10
		1.00	0.008	7
	$^4He^{2+}$	0.90	0.024	10
Cr	$^1H^+$	0.85	0.004	10
		1.00	0.007	7
	$^4He^{2+}$	0.90	0.018	10
Mn	$^1H^+$	0.81	0.003	10
		1.00	0.005	7
	$^4He^+$	0.81	0.010	10
Fe	$^1H^+$	1.00	0.005	7
	$^2H^+$	1.46	0.005	11
		1.69	0.005	
		1.77	0.004	
		2.14	0.003	
		2.35	0.003	
		2.71	0.002	
		3.03	0.002	
	$^4He^{2+}$	1.31	0.024	11
		1.46	0.023	
		1.69	0.019	
		1.77	0.016	
		2.14	0.013	
		2.35	0.012	
		2.71	0.009	
		3.03	0.007	

[a] Calculated using Eq. (2).
[b] Calculated using Eq. (1).

angement is unimportant for compounds of third-row elements when only one or two L vacancies are created in the collision.

Finally, a search of the literature was carried out to obtain a body of light-ion data sufficient to elaborate the systematic behavior of $\bar{p}_L$ as a function of relative velocity and target atomic number. The $\bar{p}_L$ values calculated using Eq. (1) and the relative intensities given in the corresponding references are listed in Table IV along with the pro-
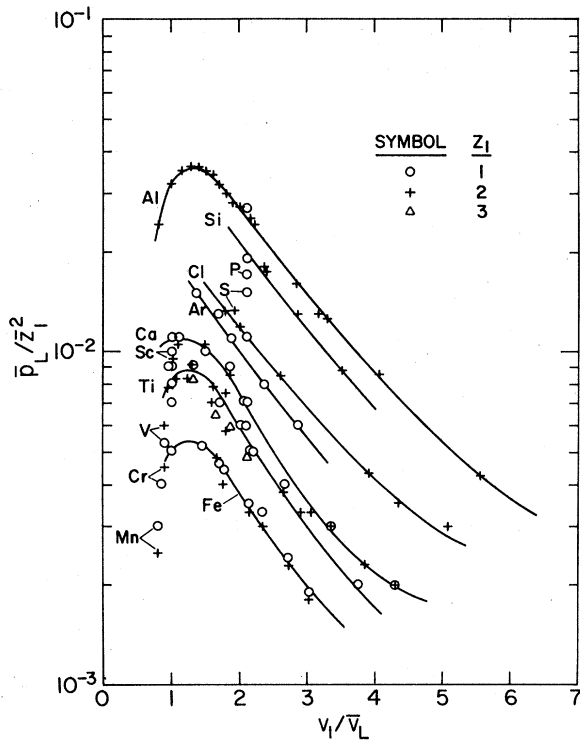
FIG. 2. Comparison of $\bar{p}_L$ values for various light-ion-projectile—target combinations as a function of relative velocity. The data shown here are listed in Table IV.

jectile to average L-electron velocity ratio (relative velocity) given by

$$v_1/\bar{v}_L = [(E/M)(m/\bar{u}_L)]^{1/2} . \qquad (2)$$

In Eq. (2), E is the projectile energy, M is the projectile mass, m is the electron mass, and $\bar{u}_L$ is the average $2s$-$2p$ electron binding energy obtained from the compilation by Bearden and Burr.[13] The data in Table IV are shown plotted as a function of $v_1/\bar{v}_L$ in Fig. 2.

III. COMPARISON WITH THEORY

Although the main features of the cross sections for ionization of K- and L- shell electrons by light ions are remarkably well described by the PWBA (plane-wave Born approximation)[14] and the BEA,[3] initial attempts at applying these theoretical methods to the description of K- plus multiple L-shell ionization have not been very successful.[1,8,10-12,15-18] In general it has been found that the BEA greatly overestimates the average L-shell ionization probability for the multiple-ionization process.

An exact definition of the average L-shell-ionization probability in K-shell-ionizing collisions may be given in terms of the cross sec-

tions for ionizing one K-shell and n L-shell electrons σ_{KL^n}:

$$\bar{p}_L = \frac{1}{8} \sum_{n=1}^{8} n\sigma_{KL^n} \bigg/ \sum_{n=0}^{8'} \sigma_{KL^n} . \qquad (3)$$

In the event that the σ_{KL^n} for $n \gtrsim 3$ are very small (as in light-ion collisions with intermediate-Z elements), the variation of the fluorescence yield may, to a good approximation, be neglected—in which case Eqs. (1) and (3) become identical. For example, the $\bar{p}_L$ values for He on Al calculated directly from measured relative intensities decrease at most by only 2% when they are recalculated from relative intensities which have been corrected using the theoretical fluorescence yields given by Richard et al.[1]

Theoretically, the required cross sections σ_{KL^n} may be computed using a model which gives the ionization probability (per electron) p as a function of impact parameter. Both the BEA[18] and SCA[4] methods provide a means of obtaining these ionization probabilities. In terms of the total ionization probability P, the multiple-ionization cross sections are given by

$$\sigma_{KL^n} = 2\pi \int_0^\infty P_{1K}(b)P_{nL}(b)b\,db , \qquad (4)$$

where b is the impact parameter. It has been customary in previous calculations of this type to treat the L electrons as if they are all ejected simultaneously (or instantaneously) and hence are subject to the same average binding energy. This view leads to the usual binomial probability terms for P_{1K} and P_{nL} in Eq. (4); namely,

$$P_n = \binom{N}{n} p^n q^{N-n} , \qquad (5)$$

where $q = 1 - p$ and N is the total number of electrons in the shell before the collision.

Another way of treating the problem is to view the L electrons as being ejected sequentially. Then the effect of the binding-energy increase which accompanies the ejection of each electron can be formally introduced into the calculation. This requires that the impact-parameter-dependent ionization probability p_i be obtained for each electron using the correct binding energy for that particular step of the sequence. Since the ionization probabilities are now not all equal, the probability distribution is no longer binomial and the total ionization probabilities p_{nL} to be used in Eq. (4) are given by the formula[19]

$$P_{nL} = \left(\prod_{i=0}^{n} p_i\right) \sum_{j=1}^{n+1} \frac{q_j^{N+1}}{\prod_{\substack{k=0 \\ k \neq j}}^{n+1} (q_j - q_k)} , \qquad (6)$$

in which $p_0 = 1$ and $q_0 = 0$. The above equation appears rather formidable, but it can be under-

stood quite simply by considering a hypothetical case in which only four L electrons are available for ionization. The total probability of not ejecting any L electrons P_0, of ejecting one and only one L electron $P_1, \ldots,$ etc., is readily seen to be

$$P_0 = q_1 q_1 q_1 q_1 = q_1^4 ,$$

$$P_1 = p_1 q_2 q_2 q_2 + q_1 p_1 q_2 q_2 + q_1 q_1 p_1 q_2 + q_1 q_1 q_1 p_1$$
$$= p_1 (q_1^3 + q_1^2 q_2 + q_1 q_2^2 + q_2^3) ,$$

$$P_2 = p_1 p_2 q_3 q_3 + p_1 q_2 p_2 q_3 + p_1 q_2 q_2 p_2 + q_1 p_1 p_2 q_3$$
$$+ q_1 p_1 q_2 p_2 + q_1 q_1 p_1 p_2$$
$$= p_1 p_2 (q_1^2 + q_1 q_2 + q_1 q_3 + q_2^2 + q_2 q_3 + q_3^2) ,$$

$$P_3 = p_1 p_2 p_3 q_4 + p_1 p_2 q_3 p_3 + p_1 q_2 p_2 p_3 + q_1 p_1 p_2 p_3$$
$$= p_1 p_2 p_3 (q_1 + q_2 + q_3 + q_4) ,$$

$$P_4 = p_1 p_2 p_3 p_4 .$$

It may be verified that the above relations for $n = 0$, 1, 2, 3, and 4 are generated by Eq. (6) with $N = 4$.

Calculations were performed for He ions on Al using both formulations (i.e. simultaneous and sequential) with BEA ionization probabilities obtained by the methods of Hansen.[18] The electron binding energies required to compute the appropriate ionization probabilities in the sequential formulation were obtained from Hartree-Fock-Slater calculations.[20] Calculations with SCA ionization probabilities obtained from the tabulations of Hansteen et al.[21] were carried out using only the simultaneous ejection formulation.

In Fig. 3, the relative total-ionization-probability distributions for the particular value $\bar{p} = 0.206$ obtained with the two distribution functions [Eqs. (5) and (6)] are compared. The most
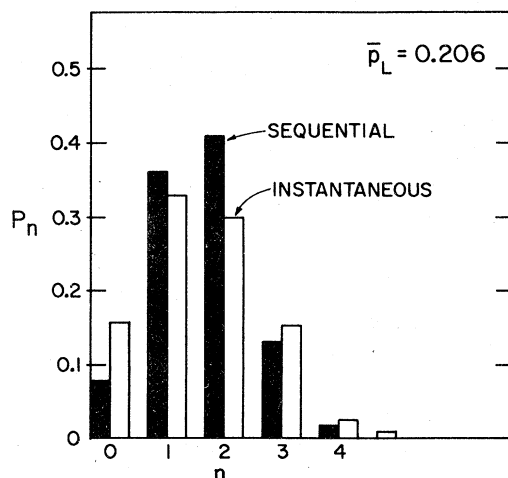
FIG. 3. Comparison of probability distributions for $\bar{p}_L$ = 0.206 calculated using the simultaneous- (or instantaneous-) and sequential-electron-ejection formulations.
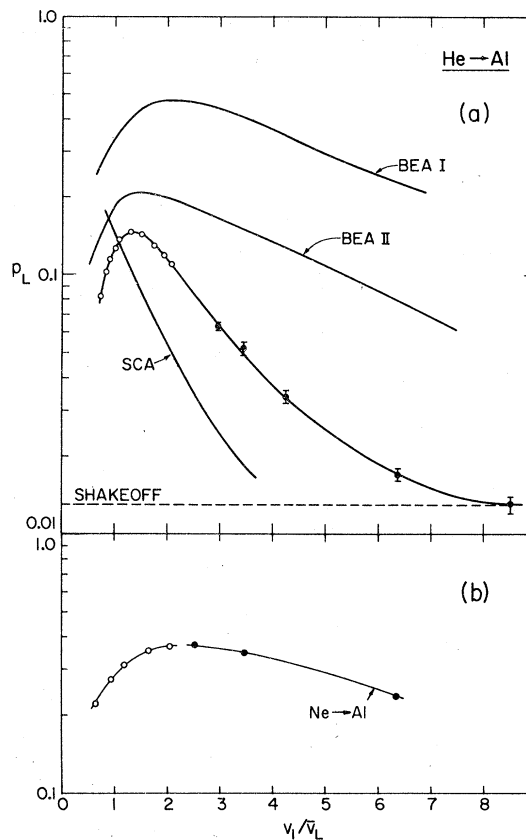
FIG. 4. (a) Experimental and theoretical velocity dependence of $\bar{p}_L$ for He ions on Al (open data points from Ref. 1). The BEA I calculation is with the simultaneous formulation and the BEA II calculation is with the sequential formulation. (b) Experimental velocity dependence of $\bar{p}_L$ for Ne ions on Al. The open data points are from Ref. 2.

evident difference between the two is that the sequential distribution is somewhat narrower in overall width than the simultaneous distribution. This characteristic is reminiscent of the narrowing which is observed in the heavy-ion induced $K\alpha$ x-ray satellite-intensity distributions for Si and S in going from the solids to the gaseous hydrides SiH_4 and H_2S, in which electron rearrangement effects occurring prior to x-ray emission are minimal.[6,22]

The velocity dependences of $\bar{p}_L$ predicted by the present calculations are compared with the experimental data for He ions incident on Al in Fig. 4(a). As observed previously, the BEA I (simultaneous ejection) calculations give $\bar{p}_L$ values which are two to five times too large. In addition, it is found that the predicted $\bar{p}_L$ values decrease much too slowly at large values of the relative velocity. The SCA calculations, on the other hand, give $\bar{p}_L$ values which are generally too small. However, the shape of the velocity

dependence at $v_1/\bar{v}_2 \gtrsim 2$ is in reasonable agreement with experiment. Recently, Aashamar and Kocbach[23] have shown that the description of final states (using only a single s state) in the treatment of Hansteen and Mosebekk[4] leads to sizable discrepancies when compared to SCA calculations using realistic (Hartree-Fock-Slater) continuum wave functions. In addition, the tabulated SCA ionization probabilities (Ref. 21) used in the present calculations were obtained with effective target atomic numbers appropriate for the calculation of binding energies rather than those which relate to the wave functions. This choice leads to large deviations from standard PWBA results for total cross sections. Calculations are currently underway using SCA ionization probabilities which have been obtained with a theoretical description that does not require the above approximations.[24]

The sequential-ejection formulation [BEA II curve in Fig. 4(b)] leads to a considerable reduction of the predicted $\bar{p}_L$ values bringing them into much better agreement with the experimental values in the region of the maximum. However, the overall shape of the curve is not greatly changed and the calculated $\bar{p}_L$ values do not exhibit the correct velocity dependence beyond the maximum.

Shown in Fig. 4(b) is the dependence of $\bar{p}_L$ on relative velocity for Ne ions on Al. The open data points are from the work of Knudson et al.[2] It is apparent that the velocity dependence observed for light ions, such as He, is considerably different than that observed for heavier ions. With He ions the $\bar{p}_L$ values exhibit a rather sharp maximum at a relative velocity of 1.25 and they decrease fairly rapidly as the relative velocity increases. At a relative velocity around 9 the data converge with the shakeoff limit as observed in photon fluorescence measurements $(\bar{p}_L = 0.013)$.[25] The Ne $\bar{p}_L$ values, on the other hand, display a very broad maximum centered about a relative velocity of 2.3 and decrease much more slowly with increasing relative velocity than do the He values. In fact, the shape of the Ne ion curve resembles that of the BEA I curve for He ions in Fig. 4(a). Of course, with Ne ions the average degree of L-shell ionization is sufficiently large so that the variation of fluorescence yield can no longer be neglected, and also these projectiles are not fully stripped ions. Hence this resemblance must be considered to be strictly fortuitous.

The dependence of $\bar{p}_L$ on target atomic number is shown in Fig. 5 for He ions at $v_1/\bar{v}_L = 2.0$. The data points were obtained from the smooth curves drawn through the data points in Fig. 2. It
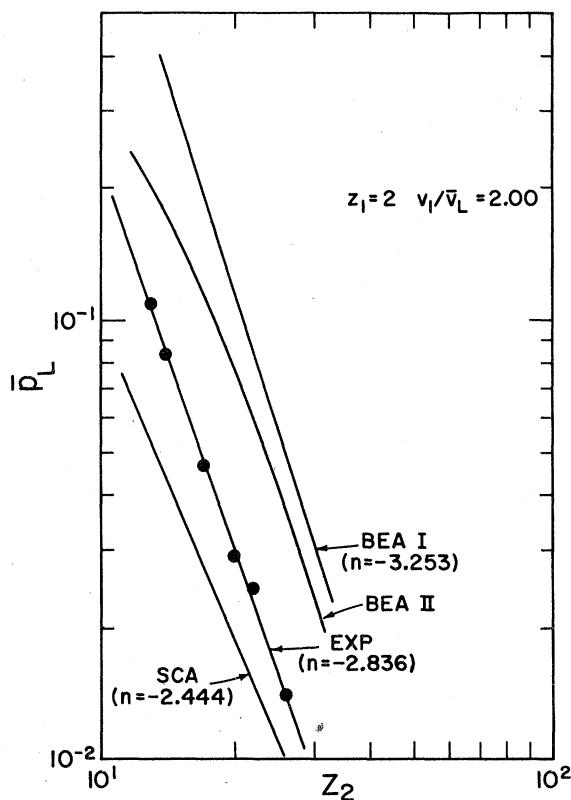
FIG. 5. Experimental and theoretical dependence of $\bar{p}_L$ on target atomic number for He ions at a relative velocity of 2.0.
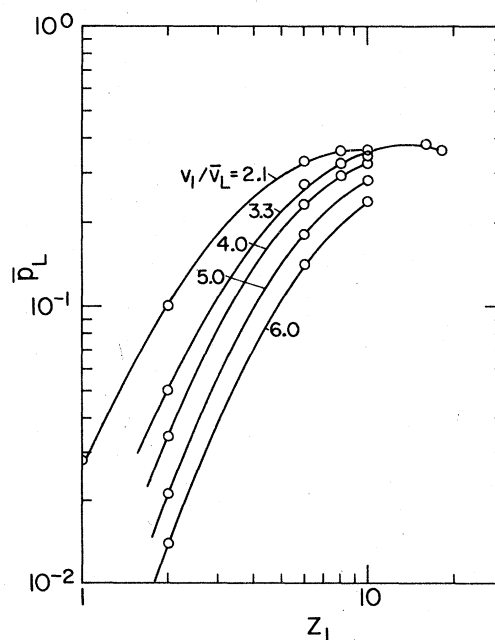
FIG. 6. Dependence of $\bar{p}_L$ for Al on projectile atomic number at several relative velocities.

is seen that the experimental Z_2 dependence may be expressed in the form of a power law

$$\bar{p}_L(Z_2) = kZ_2^n, \tag{7}$$

where the best straight-line fit gives $n = -2.836$. The BEA I and SCA calculations do, in fact, predict power-law dependences, but give $n = -2.44$ and $n = -3.25$, respectively. The BEA II results approach the power-law dependence given by the BEA I calculations at high Z_2, but depart from a simple power law below $Z_2 \simeq 22$.

IV. SEMIEMPIRICAL SCALING LAW

A particularly useful feature of the PWBA and BEA descriptions of inner-shell ionization by heavy charged particles is that they yield approximate scaling laws whereby the projectile and target atomic number dependences of the ionization cross section can be separated from the relative velocity dependence. This, in turn, enables the prediction of ionization cross sections for any projectile-target combination from a single "universal" velocity function.

Because multiple L-vacancy production is a highly probable consequence of K-shell ionizing collisions by heavy charged particles, it is desirable to have available a suitable basis for predicting its dependence on projectile and target atomic number, and on projectile velocity—especially since (as has been demonstrated in the preceding section) current theoretical descriptions are inadequate. The fact that $\bar{p}_L$ is intimately connected to the cross section for K-shell ionization suggests that a similar scaling law might also apply to this parameter.

It has been shown in Sec. III that for He ions at a relative velocity of 2.0 the dependence of $\bar{p}_L$ on target atomic number (Z_2) is well represented by a power law. The dependence of $\bar{p}_L$ for Al (at several relative velocities) on projectile atomic number (Z_1) is shown in Fig. 6. The data points in this figure have been taken from smooth curves drawn through the data given in Tables II and IV and from Ref. 8. As has been noted previously,[8] the $\bar{p}_L$ values deviate considerably from a simple power-law dependence at Z_1 greater than about 3. Even the shapes of the curves at high Z_1 in Fig. 6 vary considerably at the lower relative velocities. For light ions having $Z_1 = 1-3$, however, the dependence of $\bar{p}_L$ on Z_1 appears to be reasonably well approximated by the power law

$$\bar{p}_L(Z_1) = \bar{p}_L(Z_1 = 1)Z_1^2 \tag{8}$$

over a wide range of relative velocities.

Assuming that the Z_1 and Z_2 dependences ex-
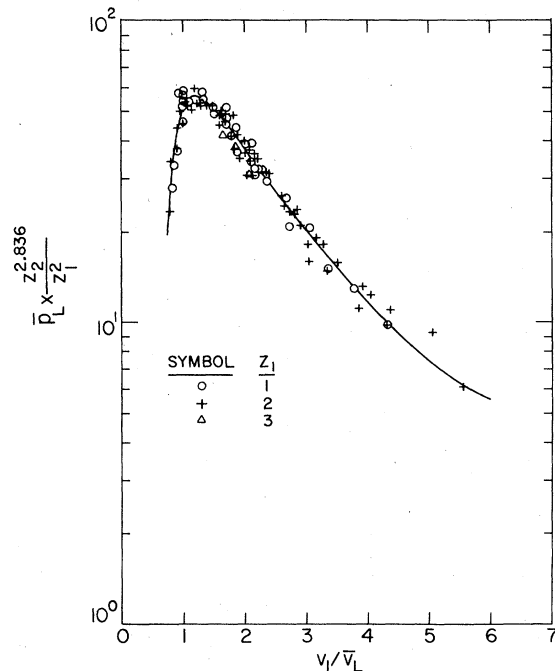
FIG. 7. Universal curve for scaled light-ion $\bar{p}_L$ values.

pressed by Eqs. (7) and (8) are essentially independent of relative velocity and are general in their applicability to multiple L-shell ionization by light ions, the complete functional dependence of $\bar{p}_L$ may be represented by an equation of the form

$$\bar{p}_L(Z_1, Z_2, v_1/\bar{v}_L) = kZ_1^m Z_2^n f(v_1/\bar{v}_L), \tag{9}$$

where $m = 2$, $n = 2.836$, and $f(v_1/\bar{v}_L)$ is a "univ-

TABLE V. Universal curve for scaled light-ion $\bar{p}_L$ values.

$v_1/\bar{v}_L$ [a]	$\bar{p}_L(Z_2^{2.836}/Z_1^2) = kf(v_1/\bar{v}_L)$
0.80	27.5
0.90	41.5
1.00	51.2
1.10	55.2
1.20	56.0
1.30	55.0
1.40	53.0
1.50	50.7
1.60	48.0
1.80	43.0
2.00	37.5
2.50	27.2
3.00	19.8
3.50	14.9
4.00	11.4
4.50	9.00
5.00	7.32
5.50	6.18

[a] Defined according to Eq. (2).

ersal" velocity function. Thus, if the above assumption about the generality of this formulation is valid, the $\bar{p}_L$ values given in Table IV, when divided by the scaling factor $Z_1^2 Z_2^{-2.836}$, should form a single curve which defines the shape of the universal velocity function.

The scaled $\bar{p}_L$ values from Table IV are shown plotted in Fig. 7. It is seen that the data all scale quite well over a wide range of relative velocities and target atomic numbers. The scaling law given by Eq. (9) therefore provides a convenient and fairly accurate means of predicting $\bar{p}_L$ values for light-ion collisions. The universal function $kf(v_1/v_L)$ shown by the smooth curve in Fig. 7 is tabulated in Table V.

As might be suspected from Fig. 4(b), the scaling law deduced for H, He, and Li ions does not hold for heavier ions such as C, O, and Ne. At $v_1/v_L \sim 2$, the scaled $\bar{p}_L$ values for C are about 50% too low and the scaled $\bar{p}_L$ values for O are

about 75% too low. However, as the velocity ratio increases, the scaled $\bar{p}_L$ values for C and O approach the universal curve established by the light-ion data. This suggests that in the limit of high projectile velocities, where (i) the projectile is full stripped, (ii) the $\bar{p}_L$ values are small enough that the effect of fluorescence yield variation is negligible and (iii) the effect of the projectile charge on the binding energies of the target *L* electrons is small, a single universal scaling law applies to both light and heavy ions.

*Present address: United States Air Force Academy, Colorado Springs, Colo.

†Present address: Air Force Weapons Laboratory, Kirtland Air Force Base, Albuquerque, N. M. 87117.

[1] P. Richard, R. L. Kauffman, J. H. McGuire, C. F. Moore, and D. K. Olsen, Phys. Rev. A **8**, 1369 (1973).

[2] A. R. Knudson, D. J. Nagel, and P. G. Burkhalter, Phys. Lett. A **42**, 69 (1972).

[3] J. D. Garcia, Phys. Rev. A **1**, 280 (1970).

[4] J. M. Hansteen and O. P. Mosebekk, Nucl. Phys. A **201**, 541 (1973); Z. Phyz. **234**, 281 (1970).

[5] R. L. Watson, A. K. Leeper, B. I. Sonobe, T. Chiao, and F. E. Jenson, Phys. Rev. A **15**, 914 (1977).

[6] J. A. Demarest and R. L. Watson, Phys. Rev. A **17**, 1302 (1978).

[7] V. Dutdiewicz, H. Bakhru, and N. Cue, Phys. Rev. A **13**, 306 (1976).

[8] R. L. Watson, F. E. Jenson, and T. Chiao, Phys. Rev. A **10**, 1230 (1974).

[9] C. Schmiedekamp, B. L. Doyle, T. J. Gray, R. K. Gardner, K. A. Jamison, and P. Richard (unpublished).

[10] R. L. Kauffman, J. H. McGuire, P. Richard, and C. F. Moore, Phys. Rev. A **8**, 1233 (1973).

[11] T. K. Li, Ph.D. dissertation (Texas A&M University, 1973) (unpublished).

[12] K. W. Hill, B. L. Doyle, S. M. Shafroth, D. H.

Madison, and R. D. Deslattes, Phys. Rev. A **13**, 1334 (1976).

[13] J. A. Bearden and A. F. Burr, Rev. Mod. Phys. **39**, 125 (1976).

[14] E. Merzbacher and H. W. Lewis, in *Encyclopedia of Physics*, edited by S. Flügge (Springer-Verlag, Berlin 1958), Vol. 34, p. 166.

[15] J. M. Hansteen and O. P. Mosebekk, Phys. Rev. Lett. **29**, 1361 (1972).

[16] T. K. Li, R. L. Watson, and J. S. Hansen, Phys. Rev. A **8**, 1258 (1973).

[17] J. H. McGuire and P. Richard, Phys. Rev. A **8**, 1374 (1973).

[18] J. S. Hansen, Phys. Rev. A **8**, 822 (1973).

[19] We acknowledge the help of T. Kishimoto of the Texas A&M Cyclotron Institute in obtaining this formula.

[20] F. Herman and S. Skillman, *Atomic Structure Calculations* (Prentice-Hall, Englewood Cliffs, 1973).

[21] J. M. Hansteen, O. M. Johnsen, and L. Kocback, At. Data and Nucl Data Tables **15**, 305 (1975).

[22] F. Hopkins, A. Little, N. Cue, and V. Dutkiewicz, Phys. Rev. Lett. **37**, 1100 (1976).

[23] O. Aashamar and L. Kocbach, J. Phys. B **10**, 869 (1977).

[24] A. Langenberg, J. F. Reading, J. R. White, and R. L. Watson (unpublished).

[25] T. Aberg, Phys. Lett. A **26**, 75 (1968).